A Letters Journal Exploring the Frontiers of Physics

October 2008

EPL, **84** (2008) 10006
doi: 10.1209/0295-5075/84/10006

www.epljournal.org

Chaotic destruction of Anderson localization in a nonlinear lattice

S. Tietsche and A. Pikovsky[(a)]

Department of Physics and Astronomy, Potsdam University - 14476 Potsdam-Golm, Germany, EU

received 16 June 2008; accepted in final form 21 August 2008
published online 19 September 2008

PACS 05.45.-a – Nonlinear dynamics and chaos
PACS 73.20.Fz – Weak or Anderson localization
PACS 63.50.-x – Vibrational states in disordered systems

Abstract – We consider a scattering problem for a nonlinear disordered lattice layer governed by the discrete nonlinear Schrödinger equation. The linear state with exponentially small transparency, due to the Anderson localization, is followed for an increasing nonlinearity, until it is destroyed via a bifurcation. The critical nonlinearity is shown to decay with the lattice length as a power law. We demonstrate that in the chaotic regimes beyond the bifurcation the field is delocalized and this leads to a drastic increase of transparency.

The Anderson localization, first studied in the context of electron transport in disordered solids [1], is a general phenomenon describing various physical situations [2,3]. Well-known examples are wave propagation in a random medium [4] and quantum chaos [5,6]. Roughly speaking, localization means that in a linear disordered system for almost all random realizations of the potential the eigenstates are exponentially localized and the spectrum is pointlike [2]. It manifests itself as a vanishing mobility of electrons, an exponentially small transparency of a random layer for waves, and a suppression of classical diffusion for quantum chaos.

Effects of nonlinearity on localization properties have attracted large interest recently. Indeed, nonlinearity naturally appears for localization of a Bose-Einstein condensate, as its evolution is described by the nonlinear Gross-Pitaevskii equation [7]. An interplay of disorder, localization, and nonlinearity is also important in other physical systems like wave propagation in nonlinear disordered media [8–10] and chains of nonlinear oscillators with randomly distributed frequencies [11,12].

In this letter we study effects of a relatively small nonlinearity on the strongly localized states (for effects of a small disorder on strongly nonlinear states see, *e.g.*, [13]). Recently it was demonstrated that an initialy concentrated wave packet spreads apparently indefinitely in a nonlinear lattice, provided the nonlinearity is strong enough [14–16]. Here we focus on another setup, namely on the *scattering* problem: we study how an incident wave is transmitted through a finite layer of a disordered nonlinear medium. Such a setup fits especially the optical experiments, where a transmission through a disordered nonlinear layer can be studied in dependence on the intensity of the incident light beam. Another physical realization is a propagation of a Bose-Einstein condensate through a waveguide with disorder [17].

We model a nonlinear disordered medium with the discrete Anderson nonlinear Schrödinger equation (DANSE)

$$i\frac{\partial \psi_n}{\partial t} = E_n\psi_n + \beta|\psi_n|^2\psi_n + \psi_{n+1} + \psi_{n-1}, \qquad (1)$$

where β characterizes nonlinearity and the on-site energies E_n (which are shifted in such a way that $E=0$ corresponds to the central energy of the band) are independent random variables distributed uniformly in the range $-W/2 < E_n < W/2$. For $\beta = 0$ all eigenstates are exponentially localized with the localization length $l \approx 96W^{-2}$ (for weak disorder) at the center of the energy band [3]. The DANSE (1) exactly describes recent experiments with one-dimensional disordered waveguide lattices (cf. eq. (1) in [10]), it also serves as a paradigmatic model for a wide class of physical problems where interplay of nonlinearity and disorder is important.

For DANSE (1) we formulate the following scattering problem. Nonlinear lattice (1) is supposed to be finite $1 \leqslant n \leqslant L$ and attached at the ends to linear regular lattices with $\beta = E = 0$ (we remind that $E=0$ corresponds to the central energy of the band). In the linear lattice attached at the left end, there is an incident wave with amplitude A and frequency ω_0: $\psi_{inc}(n,t) = A\exp[iK(\omega_0)n - i\omega_0 t]$ with $\omega_0 = 2\cos K$. We are interested in the transmission of this wave through the finite nonlinear disordered layer

[(a)] E-mail: pikovsky@uni-potsdam.de

$1 \leqslant n \leqslant L$, and particularly in the outgoing wave at $n > L$. The exact boundary conditions for a finite lattice $1 \leqslant n \leqslant L$ resulting from this setup are non-local in time, because of dispersion of linear waves in the attached lattices, they can be written as time integrals. As they are rather complex for a numerical implementation, we use below simplified boundary conditions valid for monochromatic waves, *i.e.* we neglect the dispersion:

$$\begin{aligned}(\omega_0 - e^{iK})\psi_0 &= -2i \sin K A e^{-i\omega_0 t} + \psi_1, \\ (\omega_0 - e^{iK})\psi_{L+1} &= \psi_L.\end{aligned} \tag{2}$$

This is mostly justified at the center of the band, where the dispersion is minimal, thus we set hereafter $\omega_0 = 0$, $K = -\pi/2$, and use the following model boundary conditions:

$$\psi_0 = 2A - i\psi_1, \qquad \psi_{L+1} = -i\psi_L. \tag{3}$$

(Note that these boundary conditions are time-independent, the same holds for a general ω_0 in (2) if one goes into the rotating with this frequency reference frame.) In the absence of the incident wave these conditions just describe radiation through the boundaries [18]. We stress here that these boundary conditions are approximate ones: formally they are exact for a sinusoidal wave having the central frequency of the band, by extending them to other spectral components we make an approximation that enormously simplifies numerical simulations. Possible improvements of this approximation will be studied in the future. Note that the amplitude of the transmitted wave is $|\psi_L|$. An additional constant term $2A$ describes an income of energy due to the incident wave. As a result, the lattice (1) with boundary conditions (3) is a *nonlinear driven dissipative dynamical system*. This imposes a viewpoint on the problem that is quite different from those usual in the studies of nonlinear lattices: we have to investigate attractors and their bifurcations. Possible attractors in system (1), (3) are steady states (they correspond to harmonic reflected and transmitted waves having the same frequency ω_0 as the incident one), periodic and quasiperiodic regimes (corresponding to regularly modulated reflected and transmitted waves) and chaotic attractors (corresponding to a turbulent state in the lattice layer with irregular reflected and transmitted waves; see [19] for an example of chaotization of waves at their scattering on a nonlinear impurity without disorder). We emphasize here that the dissipation in the model (1), (3) is purely radiative. Indeed, according to eq. (1) there are no internal energy losses (of course, the model can be extended for such a case as well, but this goes beyond the scope of this letter) and the only source of dissipation are boundary conditions (3) which describe the effect of the excitation of the outgoing waves in the linear lattices attached at $n = 1$ and $n = L$.

As bifurcation parameter we take the nonlinearity constant β, while keeping the amplitude of the incident wave constant, $A = 1$. These two parameters are of course equivalent via a rescaling, thus an increasing of β is equivalent to an increasing of the amplitude of the incident wave. Particularities of attractors and their bifurcations depend on the realization of the random potential $\{E_n\}$, therefore to achieve general conclusions we will perform below a *statistical bifurcation analysis* of problem (1), (3); in this aspect our approach differs from direct numerical simulations of a nonlinear scattering problem in [17]. We will consider the system length L as another essential parameter of the problem; the distribution of energies will be hereafter fixed $-2 \leqslant E_n \leqslant 2$. The range of the disorder is chosen to be equal to the band width, so this disorder is neither weak nor strong.

Because of the symmetry of this distribution we can restrict our numerical analysis to the case of positive β only. Indeed, with the "staggered" transformation $\psi_n = (-1)^n \phi_n^*$ one transforms (1), (3) to

$$\begin{aligned}i\frac{\partial \phi_n}{\partial t} &= -E_n\phi_n - \beta|\phi_n|^2\phi_n + \phi_{n+1} + \phi_{n-1}, \\ \psi_0 &= 2A - i\phi_1, \qquad \psi_{L+1} = -i\phi_L,\end{aligned}$$

which is equivalent to (1), (3) if one changes signs of E_n and β. Because the distribution of E_n is symmetric, statistical properties of bifurcations do not depend on the sign of β, although for a particular disorder realization the sign of nonlinearity is relevant.

Our starting point is the linear case $\beta = 0$. Here the dissipative system (1), (3) has a unique global attractor: a stationary state. This state corresponds to the unique solution of the linear scattering problem. The amplitude in this state decreases in average exponentially with the index n, so that the transmitted wave for large L is exponentially small $|\psi_L| \sim \exp(-L/l)$. This is just the manifestation of the Anderson localization in the context of the scattering setup. This state, as well as its stability properties, can be easily found numerically. Expectedly, but nevertheless remarkably, the linear state becomes less stable with the increase of the layer length L. The system (1), (3) has $2L$ complex eigenvalues $\mathrm{Re}(\lambda_k) + i\mathrm{Im}(\lambda_k)$, all of them have negative real parts, so the amplitudes of the perturbations decay $\sim \exp(\mathrm{Re}(\lambda_k)t)$. In fig. 1 we show the distributions of the closest to zero real part $\mathrm{Re}(\lambda_0)$, for different system lengths, this quantity determines the slowest decay rate. One can see that for larger L the real part of the eigenvalue becomes exponentially close to zero, because the coupling of localized modes at the middle part of the layer with the boundaries is exponentially weak. We will see that these weakly damped modes dominate the bifurcations when the nonlinearity is increased.

Starting with the stable steady state at $\beta = 0$, we followed this state for an increasing β, until this state bifurcates at some β_c. We have performed the bifurcation analysis [20] automatically for about 10^4 realizations of the random potential, and summarize the results for different lengths of the layer in fig. 2. The maximal value of β in the analysis was $\beta = 2$. If the steady state remains stable up to

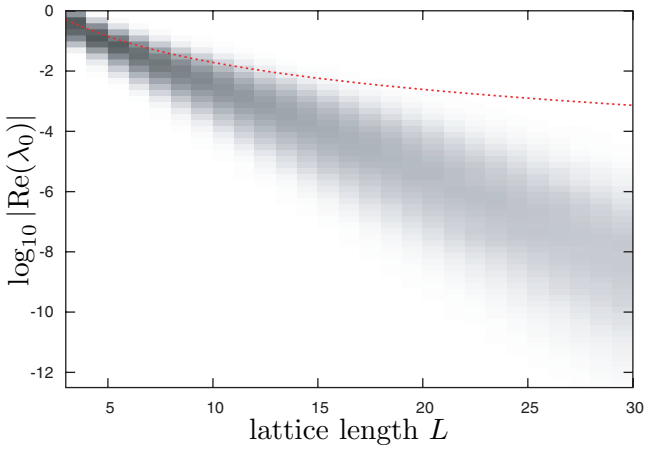

Fig. 1: (Color online) A gray scale plot of distributions of the eigenvalues λ_0 with the largest real part for different lattice lengths, obtained from an ensemble of 10^4 realizations of random potential, black indicates high probability. The dashed line shows the value of λ_0 for a regular linear lattice.

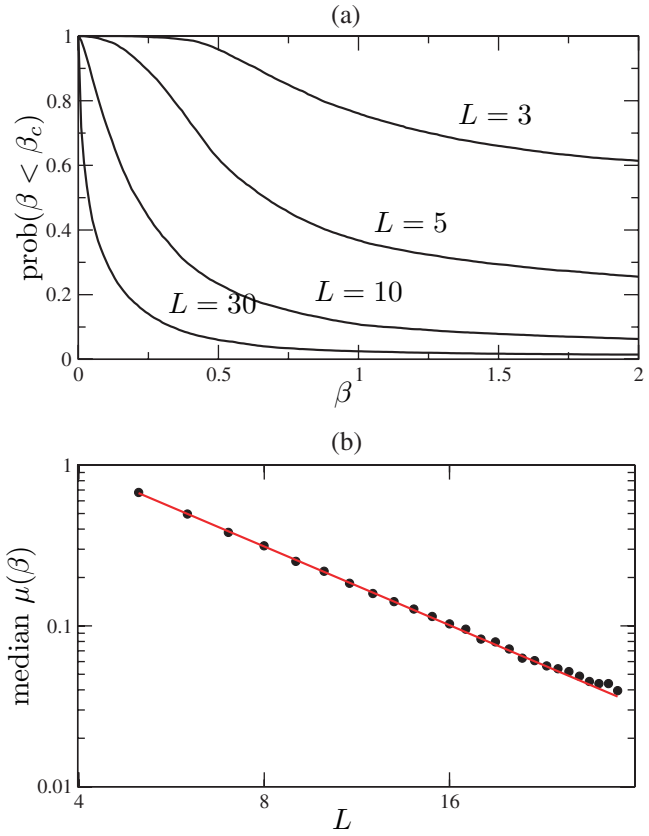

Fig. 2: (Color online) (a): Cumulative distributions of the critical nonlinearity values, the curves show the probability that $\beta_c > \beta$. (b): Dependence of the median $\mu(\beta)$ of the distribution (defined as $\mathrm{prob}[\beta_c > \mu(\beta)] = 1/2$) on lattice length L. The line is the power law $\mu(\beta_c) \approx 9.2 L^{-1.6}$.

this point, we indicate this realization of disorder as "non-bifurcating". We show the cumulative distributions of the values of β_c in fig. 2(a) for different lengths of the lattice L.

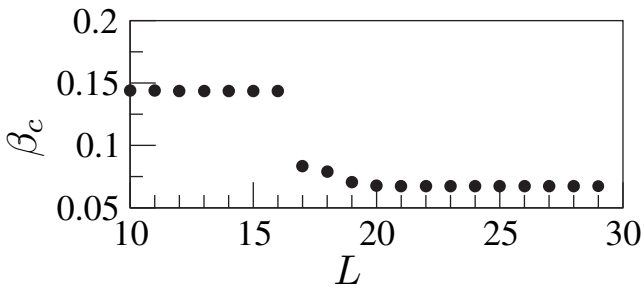

Fig. 3: The critical values of nonlinearity *vs.* system length for a particular realization of random energies (here the transition is of fold type). The corresponding field profiles and eigenmodes are shown in fig. 4.

One can see that the characteristic values of critical β_c decrease with the system length. In fig. 2(b) we conclude from the log-log plot of the median of the distribution, that the critical nonlinearity follows the power law

$$\beta_c \propto L^{-1.6}\,. \tag{4}$$

The type of the bifurcation also changes with the system length. *E.g.*, for $L = 5$ a fold (saddle-node) bifurcation (where one real eigenvalue changes sign) dominates (41.3% of all cases) over a Hopf bifurcation (31.9%), while in 26.8% of realizations no bifurcation happened until $\beta = 2$. For $L = 10$ the corresponding numbers are: 55.3% for Hopf, 38.1% for fold and 6.6% for non-bifurcating. For a longer layer $L = 30$ a Hopf bifurcation becomes predominant with 84.3%, followed by a fold one (14.3%), and only in 1.4% of all realizations no bifurcation occurs.

To obtain more insight into the properties of the critical bifurcating mode, we follow the bifurcation for one particular realization of the random potential, for different lattice sizes. After determining the bifurcation for a lattice size L, we add one additional random site to the lattice and determined the bifurcation for $L+1$, etc. The resulting values of the critical parameter are shown in fig. 3. One can see that the value of β_c drops at $L = 17$. As is illustrated in fig. 4, at this system length a change of the critical eigenmode occurs. While the critical modes for $L = 10$ and $L = 16$ are very much similar, the mode that first becomes unstable is different for $L = 17$ and $L = 23$. As with the increasing of the lattice length L more and more modes with exponentially small real parts of the eigenvalues appear, these modes become potentially dangerous for the loss of stability. As a result, for larger lattice length the bifurcation occurs for smaller nonlinearities. This qualitatively explains fig. 2 and relation (4).

We now turn to the analysis of the post-bifurcation dynamics in the lattice, that strongly depends on the type of the bifurcation. A fold bifurcation is non-local, in this case a new attractor in the system is generally quite different from the stable steady state prior to the bifurcation. The same is valid for a subcritical Hopf bifurcation, while for a supercritical Hopf bifurcation a

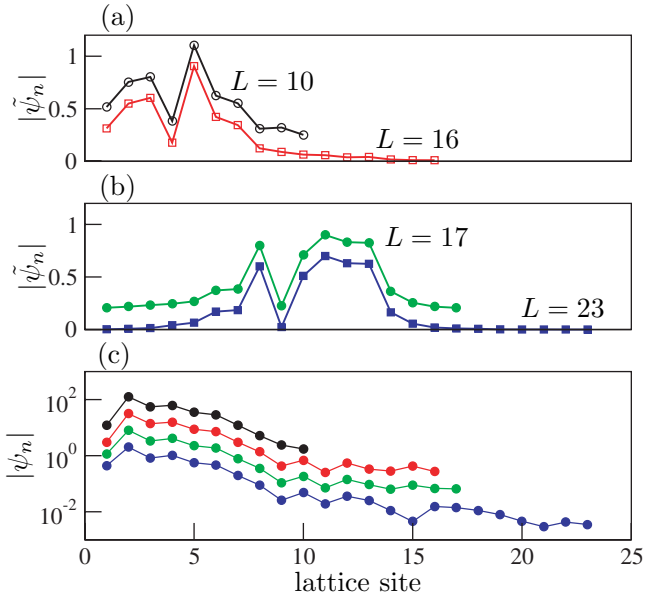

Fig. 4: (Color online) "Evolution" of the critical steady state (c) and of the critical modes $|\tilde{\psi}_n|$ [(a) and (b)] with the growing lattice length. The curves in all panels are vertically shifted for better visibility. At $L = 17$ a transition for a new critical mode located at the sites $8 \lesssim n \lesssim 15$ happens.

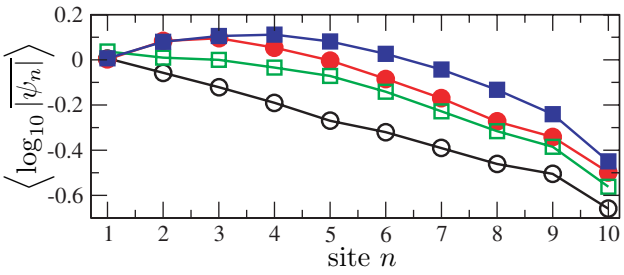

Fig. 5: (Color online) Time- and ensemble-averaged profiles of the field in the lattice of length $L = 10$ in slightly supercritical states. Open circles: linear regime; filled circles: nonlinear static regimes; open squares: periodic regimes; filled squares: chaotic regimes. All nonlinear regimes are less localized compared to the static linear state prior to bifurcation. Note that the averaging is performed for different nonlinearities, as for different realization the values of β_c differ.

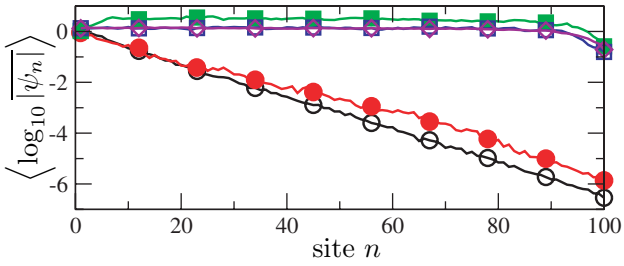

Fig. 6: (Color online) Time- and ensemble-averaged profiles of the field in a long lattice $L = 100$. Bottom curve, open circles: linear case; filled circles: periodic solutions for $\beta = 0.1$; filled squares: chaotic solutions for $\beta = 0.1$; open squares: periodic solutions for $\beta = 1$; open diamonds: chaotic solutions for $\beta = 1$; the latter two curves are almost indistinguishable.

stable periodic orbit close to the steady state appears. This distinction is crucial for experiments: at an adiabatic increase of the intensity of an incident wave, one will observe a drastic change in the outgoing wave for a non-local transition, while for a supercritical bifurcation the transition will be continuous. Furthermore, we cannot exclude multistability in the system, because new attractors can appear already for small nonlinearities $\beta < \beta_c$. We studied the post-bifurcation regimes by solving the initial-value problem (1), (3) for a slightly supercritical nonlinearity $\beta = 1.01\beta_c$, starting from the initial conditions in the vicinity of the just having become unstable steady state. For $L = 10$, of overall 10^4 realizations we observed steady states in 33% of the situations, stable periodic/quasiperiodic orbits in 59% and chaos in 8% of all cases. The classification of the attractors was performed by calculating the largest Lyapunov exponent of the solutions on the attractor in the system (1), (3), which in the three cases above was negative, zero, or positive, respectively. For all these different types of attractors we calculated the time average of the field $\overline{|\psi_n|}$ for each lattice site, and then averaged the logarithm of this time average over many realizations of the random energies. The resulting profiles are shown in fig. 5 together with the averaged static profile prior to the bifurcation. We see that the periodic post-bifurcation regimes are mostly localized, because a periodic orbit appearing at a supercritical Hopf bifurcation is mostly close to the pre-bifurcation steady state. The strongest delocalization demonstrate chaotic regimes. We stress here that the averaging in fig. 5 have been performed for different absolute values of nonlinearity β but for the same values of nonlinearity relative to the critical one $\beta/\beta_c = 1.01$. We have chosen such a conditional averaging to characterize regimes close to the transition, while the transition point itself strongly fluctuates making the averaging at a constant β less meaningful.

Unfortunately, it is extremely difficult to perform a precise bifurcation analysis as described above for really long nonlinear lattices. The reason is the mentioned above exponentially weak damping of modes, resulting in a very high sensitivity of the numerical bifurcation algorithms. Therefore we have performed for $L = 100$ a direct simulation of the initial-value problem (1), (3), starting from the "empty" lattice $\psi_n(0) = 0$. For fixed nonlinearity levels $\beta = 0.1$ and $\beta = 1$, after sufficiently long transients we first determined the types of the attractors according to the largest Lyapunov exponent, and then separately averaged the fields, like described above, for periodic and chaotic attractors (no static states were observed for such large lattices, cf. [17]). We underline that we have not studied multistability of states in each particular lattice, different states at the same nonlinearity "co-exist" in different lattices with different realizations of disorder. The results are shown in fig. 6. While for a

small nonlinearity periodic regimes are almost as localized as linear ones, for large nonlinearities there is only a weak difference between periodic and chaotic regimes. The latter ones are strongly delocalized for both nonlinearities. This means that an appearance of chaos leads to a turbulent (*i.e.* a high-dimensional chaotic state whose statistical properties practically do not depend on the system length) state in a lattice that results in an effective equipartition between modes. Only at the right end of the lattice the radiation through this boundary leads to a depletion of the profile. The transmission coefficient becomes length independent, allowing us to name this state the chaos-induced self-transparency of the disordered nonlinear lattice.

The findings presented in figs. 5, 6 can be summarized as follows. For a particular realization of the disorder in a lattice of fixed length, one observes, in dependence on the nonlinearity parameter β, three regimes. i) The regime of static localization prior to the critical value β_c. Here the field distribution is very close to that in the linear lattice. Correspondingly, one can characterize it with the linear localization length l, so that the transparency of the layer decreases in average exponentially with the lattice length: $\sim\exp(-L/l)$. ii) Just above the critical value β_c an intermediate state is observed, whose properties heavily depend on the type of the bifurcation and on other parameters. We were able to identify this state for relatively small lattices only, therefore we cannot characterize it with, *e.g.*, an effective localization length because the latter is defined asymptotically for large lattices only. In this state the transparency is larger than in the static state. Finally, for larger nonlinearities a turbulent state iii) arises as shown in fig. 6. Here the average transparency becomes finite and system-size independent. Therefore, one can attribute to this state an infinite localization length. Thus the destruction of Anderson localization can be viewed as a drastic increase of transparency of the layer or, equivalently, as a divergence of the localization length.

We have restricted our numerical experiments to a particular distribution of the on-site energies in the lattice. Several calculations for a different range of the distribution have shown only a quantitative, not a qualitative difference. A full statistical analysis in dependence on different disorder distributions (what means also different linear localization lengths) needs enormous numerical efforts and will be presented elsewhere.

In conclusion, we have formulated the scattering problem for a disordered nonlinear layer as a bifurcation problem for a nonlinear dissipative system. A static localized regime, very similar to the linear one, exists up to a critical nonlinearity that depends on the disorder realization and in average decreases with the lattice length as the power law $\beta_c \propto L^{-1.6}$. Beyond this critical value different attractors can be observed, corresponding to different regimes of transparency. In short lattices we separately averaged the three classes —static, periodic, and chaotic— of states just beyond the critical point, and have found that periodic states are more strongly localized than static and chaotic ones. In long lattices for chaotic regimes we observe an almost equidistribution of the field along the lattice with a drastically increased transmission through the layer. These regimes appear to be dominant for relatively large nonlinearities.

* * *

We thank N. Brilliantov, S. Flach, T. Paul, P. Schlagheck, and D. Shepelyansky for useful discussions.

REFERENCES

[1] Anderson P. W., *Phys. Rev.*, **109** (1958) 1492.
[2] Lifshitz I. M., Gredeskul S. A. and Pastur L. A., *Introduction to the Theory of Disordered Systems* (Wiley, New York) 1988.
[3] Kramer B. and MacKinnon A., *Rep. Prog. Phys.*, **56** (1993) 1469.
[4] Sheng P., *Introduction to Wave Scattering Localization and Mesoscopic Phenomena* (Springer, Berlin) 2006.
[5] Fishman S., Grempel D. R. and Prange R. E., *Phys. Rev. A*, **36** (1987) 289.
[6] Chirikov B. V., Izrailev F. M. and Shepelyansky D. L., *Physica D*, **33** (1988) 77.
[7] Dalfovo F., Giorgini S., Pitaevskii L. P. and Stringari S., *Rev. Mod. Phys.*, **71** (1999) 463.
[8] Skipetrov S. E. and Maynard R., *Phys. Rev. Lett.*, **85** (2000) 736.
[9] Schwartz T., Bartal G., Fishman S. and Segev M., *Nature*, **446** (2007) 52.
[10] Lahini Y., Avidan A., Pozzi F., Sorel M., Morandotti R., Christodoulides D. N. and Silberberg Y., *Phys. Rev. Lett.*, **100** (2008) 013906.
[11] Dhar A. and Lebowitz J. L., *Phys. Rev. Lett.*, **100** (2008) 134301.
[12] Zavt G. S., Wagner M. and Lütze A., *Phys. Rev. E*, **47** (1993) 4108.
[13] Gredeskul S. A. and Kivshar Y. S., *Phys. Rep.*, **216** (1992) 1.
[14] Molina M. I., *Phys. Rev. B*, **58** (1998) 12547.
[15] Pikovsky A. S. and Shepelyansky D. L., *Phys. Rev. Lett.*, **100** (2008) 094101.
[16] Kopidakis G., Komineas S., Flach S. and Aubry S., *Phys. Rev. Lett.*, **100** (2008) 084103.
[17] Paul T., Leboeuf P., Pavloff N., Richter K. and Schlagheck P., *Phys. Rev. A*, **72** (2005) 063621.
[18] Livi R., Franzosi R. and Oppo G.-L., *Phys. Rev. Lett.*, **97** (2006) 060401.
[19] Pikovsky A. S., *Chaos*, **3** (1993) 505.
[20] Kuznetsov Y., *Elements of Applied Bifurcation Theory*, in *Appl. Math. Sci. Ser.*, Vol. **112** (Springer) 1995.